Int J Earth Sci (Geol Rundsch) (2006) 95: 841–853
DOI 10.1007/s00531-005-0065-3

ORIGINAL PAPER

S-S. Xu · A. F. Nieto-Samaniego · S. A. Alaniz-Álvarez
L. G. Velasquillo-Martínez

Effect of sampling and linkage on fault length and length–displacement relationship

Received: 2 April 2003 / Accepted: 24 November 2005 / Published online: 4 January 2006

Abstract The power-law exponent (n) in the equation: $D = cL^n$, with D = maximum displacement and L = fault length, would be affected by deviations of fault trace length. (1) Assuming $n = 1$, numerical simulations on the effect of sampling and linkage on fault length and length–displacement relationship are done in this paper. The results show that: (a) uniform relative deviations, which means all faults within a dataset have the same relative deviation, do not affect the value of n; (b) deviations of the fault length due to unresolved fault tip decrease the values of n and the deviations of n increase with the increasing length deviations; (c) fault linkage and observed dimensions either increase or decrease the value of n depending on the distribution of deviations within a dataset; (d) mixed deviations of the fault lengths are either negative or positive and cause the values of n to either decrease or increase; (e) a dataset combined from two or more datasets with different values of c and orders of magnitude also cause the values of n to deviate. (2) Data including 19 datasets and spanning more than eight orders of fault length magnitudes (10^{-2}–10^5 m) collected from the published literature indicate that the values of n range from 0.55 to 1.5, the average value being 1.0813, and the peak value of n_d (double regression) is 1.0–1.1. Based on above results from the simulations and published data, we propose that the relationship between the maximum displacement and fault length in a single tectonic environment with uniform mechanical properties is linear, and the value of n deviated from 1 is mainly caused by the sampling and linkage effects.

S-S. Xu · L. G. Velasquillo-Martínez
Eje Central Lázaro Cárdenas, Instituto Mexicano del Petróleo, No. 152, Col. San Bartolo Atepehuacan, 07730 México, México

A. F. Nieto-Samaniego · S. A. Alaniz-Álvarez · S-S. Xu (✉)
Centro de Geociencias, Universidad Nacional Autónoma de México, Apartado Postal 1-742, 76001 Querétaro, México
E-mail: xshunshan@yahoo.com

Keywords Fault length · Fault displacement · Power-law exponent · Fault linkage · Sampling · Simulation

Introduction

In previous studies, the relationship between the maximum displacement (D) and length (L) of faults in the two-dimensional space has been proposed in the form

$$D = cL^n \quad (1)$$

where c is a constant related to material properties of the host rocks. A range of values of n from 0.5 to 2.0 has been reported by previous authors (e.g. Bonnet et al. 2001). The lack of consensus about the value of n may derive from large scatter of D–L data (Cowie and Scholz 1992a; Gillespie et al. 1992; Cartwright et al. 1995; Acocella et al. 2000). Deviations of fault length can be attributed to both sampling methods and the geologic processes during faulting (Cowie and Scholz 1992a; Bonnet et al. 2001). Walsh and Watterson (1988) interpreted that $n = 2$, which is consistent with a simple growth model where the slip in successive events increases by an equal increment. Marrett and Allmendinger (1991), studying a combined dataset, obtained $n = 1.5$. Gillespie et al. (1992) made synthetic analysis and also concluded that $n = 1.5$ is preferred value, which is consistent with each slip event proportional to $L^{0.5}$.

Cowie and Scholz (1992a, b) argued that $n = 1$, which can be predicted by Dugdale's fracture model. Dawers et al. (1993) published a dataset with 15 faults from the Volcanic Tableland, locating in northern Owens Valley between the Sierra Nevada and White Mountains, and obtained a linear relationship between maximum displacement and fault length, with error of measurement less than a few percent. A value $n = 0.93$ was obtained by a dataset with 237 faults measured by Mansfield and Cartwright (2001) using physical modeling. Schlische

et al. (1996) measured a dataset with 201 faults in the Mesozoic Dan River rift basin. The best-fit power-law curve for this dataset has an exponent of 0.91, which is nearly linear. The data published by Lu et al. (1989), Wen et al. (1990), and Xu et al. (1998) also indicate that the value of n is equal to 1. So there is no consensus, but most authors agree that $n=1$.

Power-law exponent (n) for D–L is important for explaining faulting mechanisms. However in many cases, the value of n is obtained from data only including two to three orders of magnitude and having measurement errors, so individual dataset could not represent the real value of n. In this paper, influences of fault length deviations on D–L relationship by mathematic models are simulated by assuming $n=1$; 19 datasets from published literature are collected and a preferred value of n is determined. The reasons of causing deviation of the value of n are also discussed.

Terminology used in this paper

Ideal fault length (L)

The slip surface of an unrestricted isolated normal fault developed in a single regime with uniform mechanical host-rock properties is taken to be an elliptical plane with the slip vector parallel to the short axis of the ellipse and symmetrical slip distribution; the slip maximum is assumed in the center of the ellipse (e.g. Barnett et al. 1987; Walsh and Watterson 1989). In this case, the fault length measured in the weathered surface is not the maximum value. When faults reach or originate in the surface and are then restricted, the slip surfaces are semi-ellipses (Dawers et al. 1993). In this case, the fault length measured in the surface is the maximum value if there is no erosion. The larger dimension of fault surface is consistent with the propagation direction of the faults, and is normal to the "controlling dimension" of Gudmundsson (2000); then, in the case of normal and thrust faults, the long axis of the ellipse is parallel to the strike of the fault. In the case of strike-slip fault, the long axis of the ellipse is parallel to the dip direction of the fault (Fig. 1). The ideal fault length (L) in this paper is defined as the long axis of the ellipse of fault surface developed in a uniform host rock during a single tectonic event.

Measured fault length (L_d)

The slip surfaces of geological faults seldom conform to that of an ideal isolated fault because of different processes of fault growth and sampling dimensions. The measured fault length may be either deviated from or equal to the long axis (L) of an ideal ellipse (unrestricted faults) or semi-ellipse (restricted faults) of the fault surface.

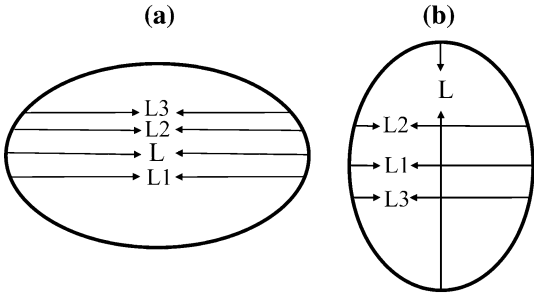

Fig. 1 Ideal fault surface of unrestricted isolated fault. In the case of normal fault (**a**), the long axis of ellipse of the fault surface is parallel to the horizontal surface. Trace lengths observed in levels 1, 2, 3 are smaller than the long axis length L. In the case of strike-slip fault (**b**), the short axis of ellipse of the fault surface is parallel to horizontal surface. The fault trace lengths ($L1$, $L2$, and $L3$) observed in the horizontal surfaces will smaller than the long axis of ellipse (L)

Absolute deviation (δ)

The absolute deviation (δ) is defined as $L_d - L$ for this paper. When the fault length is underestimated, the value of δ is less than zero; when the fault length is overestimated, the value of δ is larger than zero. Specially, when L_d has no deviation, the value of δ will be equal to zero. Evidently, for $\delta<0$, smaller values of δ result from larger deviations of the fault length.

Relative deviation (λ)

The parameter λ is defined as δ/L in this paper. When the fault length is underestimated the value of λ is less than zero; when the fault length is overestimated the value of λ is larger than zero, when the fault length has no deviation, the value of λ is equal to zero. Similar to δ, for $\lambda<0$, smaller values of λ result from larger deviations of the fault length.

Deviation analysis of fault trace length

Deviation due to limitation of observed dimension (δ_1, λ_1)

The fault trace length is generally measured in map view, which causes values of L_d to be inaccurate. In some cases, the fault did not nucleate near the surface, and in the field the observed faults outcrop correspond to the erosion level. The plane of denudation generally does not exactly include the long axis of the ellipse of fault surfaces in the case of a normal fault. This would cause underestimation of the fault trace length (Fig. 1). In the case of strike-slip fault, the measured fault length is always equal or smaller than the short axis of the ellipse fault surfaces.

On the other hand, the slip directions of oblique-slip faults are neither in the dip direction nor in the strike

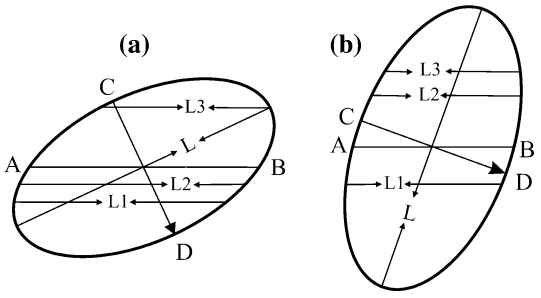

Fig. 2 Diagram showing deviation of slip direction for oblique fault with mainly normal component (**a**) and strike-slip component (**b**). In the case of (**a**), the measured maximum length *AB in the horizontal surface* is smaller than the long axis of ellipse (*L*). In the case of (**b**), all measured lengths of the fault trace in the horizontal surfaces are smaller than the long axis of ellipse (*L*). The *arrow on line CD* shows the slip direction on the fault plane

direction; then, the axes of elliptical plane are not parallel to the horizontal surface, which would cause more complicated measured fault length (Fig. 2). In Fig. 2a, arbitrary trace lengths *L*1, *L*2, *L*3 are smaller than the long axis *L*, which causes underestimation of trace length ($\delta_1 < 0$, $\lambda_1 < 0$) when the data are measured on maps that intersect different levels of the fault. In Fig. 2b, the slip direction is not the strike direction, and the short axis (CD) is not parallel to the horizontal surface, so measured fault lengths may be larger than the short axis, for example the line AB, but are always smaller than the long axis ($\delta_1 < 0$, $\lambda_1 < 0$).

Deviation due to unresolved fault tip (δ_2, λ_2)

The tip zones of faults cannot be detected when the fault displacement is below the resolution of certain observation techniques (Yielding et al. 1996; Watterson et al. 1996; Pickering et al. 1996). Different methods have different resolution limits. In the field, the observation resolution of fault displacements may reach the millimeter scale. The resolution in coalfields is in the order of centimeters (Watterson et al. 1996). Seismic resolution is typically from 15 to 30 m (Yielding et al. 1996; Pickering et al. 1996). Obviously the datasets from fieldwork have

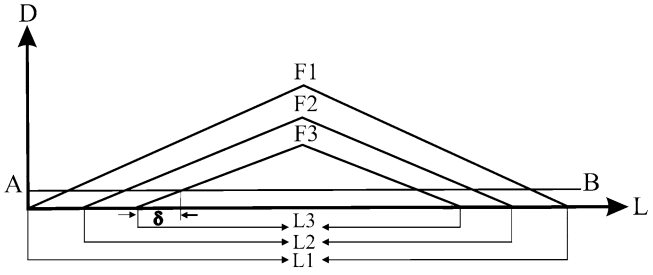

Fig. 3 Diagram showing deviations for different faults of magnitude. It is assumed that the observation resolution of displacement (line AB = δ) used a certain technique which is same for all faults. Therefore, the absolute deviation for faults *F*1, *F*2, *F*3 is equal to 2δ. The absolute values of relative deviations (λ) for small faults (e.g. *F*3) are larger than that for large fault (e.g. *F*1)

minimum deviations. The absolute value of relative deviations of trace length for small faults is larger than that for large faults while using a same observation technique (Fig. 3).

Deviation due to fault linkage

Deviation due to relay structure (soft linkage, δ_3, λ_3)

Two types of fault linkage have been proposed: soft linkage and hard linkage. Walsh and Watterson (1991) proposed that a soft linkage may exist, when the distance separating the segments is approximately an order of magnitude less than the individual segment lengths. According to Sneddon and Lowengrub (1969), the "soft linkage" has no physical justification, but it was verified by the numerical model (Cride and Pollard 1998). Whether a fault attracts or repels other faults depend on the position of the fault in the stress field of other faults (e.g. Gudmundsson et al. 1993; Gupta and Scholz 2000).

Segmented geometry is a basic property of faults. There may be developed a relay structure when one fault approaches or overlaps another fault (Willemse et al. 1996). Overlapping zones commonly have hook shape (Acocella et al. 2000). A jog zone will form in the case where linkage occurs between two faults (Peacock and Sanderson 1994; Willemse et al. 1996). The displacement distribution on segmented faults may be different from that of the isolated faults. Firstly, the maximum displacement deviates to the center of a fault segment (Willemse et al. 1996). Secondly, the displacement gradients change near the relay zones. In the case of an underlapping tip zone (Fig. 4a, c), the displacement gradients becomes steeper (Fig. 4d; also Peacock and Sanderson 1991). In the case of overlapping (Fig. 4b, e), segments show steeper displacement gradients and the maximum displacement point is closer to the overlapping end, however near the tips of fault, the displacement gradients decrease (Fig. 4f; also Dawers and Anders 1995).

In the case of underlapping, steeper gradients produce a shorter trace length than that of an isolated fault as shown in Fig. 4d. In Fig. 4d, AB is the absolute deviation when a relay structure exists. In the case of overlapping, the trace length of the segmented fault also decreases (Fig. 4f). One can see that both underlapping and overlapping structures result in segments having a smaller length than an isolated fault. Therefore some authors have suggested that segmented fault geometries would contribute to scatter for displacement-fault trace data (Peacock and Sanderson 1991; Gillespie et al. 1992; Cartwright et al. 1995; Acocella et al. 2000).

Deviation due to hard linkage (δ_4, λ_4)

Hard-linked systems are those whose individual segments are physically joined in the section studied. For

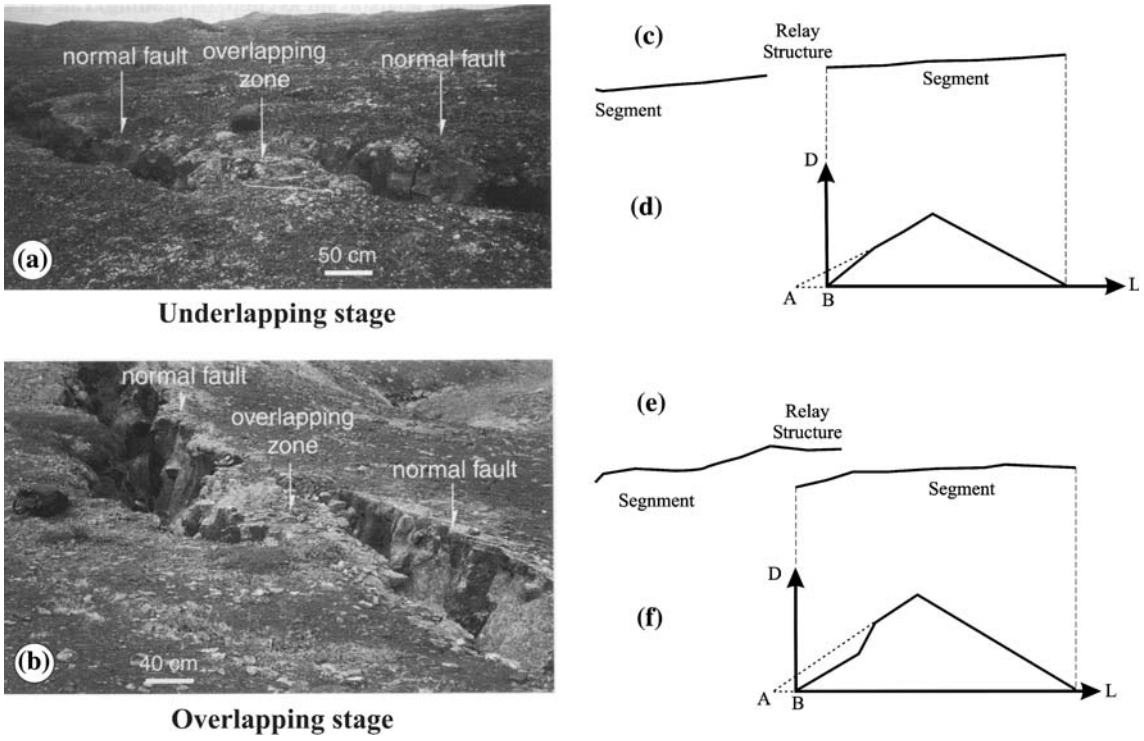

Fig. 4 Diagram of relay structure and diagram showing change of gradients of displacement near the end of relay structure. Photos (**a**) and (**b**) are from Acocella et al (2000). *AB* in (**d**) and (**f**) is absolute deviation of the fault length due to relay structure

hard linkage, Mansfield and Cartwright (2001) recognized two linkage styles: accidental linkage and incidental linkage (also Childs et al. 1995). The linkage of faults is proposed to have three stages (Acocella et al. 2000): underlapping stage, overlapping stage (soft linkage), and linkage stage (hard linkage).

There are two types of model for explaining fault linkage. One model predicts that a decrease in displacement accumulation near the interacting region is because of a locking effect prior to hard-linking (e.g. Peacock and Sanderson 1991). For this model, in the region of linked segment tips the sum of displacements is generally less than that on the adjacent parts of the fault surface. Therefore, the displacement profile may show multipeaks at the beginning of the linking. If growth follows without further linkage, the displacement profile will be similar to the simple one (Fossen and Hesthammer 1997). Crider and Pollard (1998) documented this growth model using a three-dimensional numeral experiment. A physical experiment by Mansfield and Cartwright (2001) also supported this model. Many field data (Ferrill et al. 1999; Peacock 1991; Huggins et al. 1995; Fossen and Hesthammer 1997) are also consistent with this model. The model predicts that the fault length would be overestimated (Fig. 5a–f), as well as be underestimated. Figure 5g, h shows the possibility of underestimating of fault length.

The second model has been proposed by Gupta and Scholz (2000). They argued that as linkage and coalescence occur, displacement accumulation may be concentrated near the center of the fault plane or in the overlap zone, so when linkage is completed, the displacement profile is appropriate for a single new fault. The model predicts neither over- nor underestimating of fault length.

Numerical simulation

Construction of datasets

The above analysis indicates that the deviations of trace length are complicated, and strongly influence the relationship between maximum displacement and maximum length. The distributions of displacement and length obey the power-law distribution

$$N \propto r^{-\beta}, \tag{2}$$

where N is the number equal to or greater than the size (r) of fault length (L) or displacement (D), and β is power-law exponent. For two-dimensional datasets of fault length, values of β change from 1 to 2 (Fig. 6). The largest β could be larger than 2 (e.g. Cladous and Marrett 1996). Sammis et al. (1987) proposed a simple model explaining the power-law distribution of fault segments. The model assumes that two diagonally opposed blocks are retained after repeated tensile splitting of grains and predicts that $\beta = 1.58$ for a two-dimensional configuration. This model has been applied

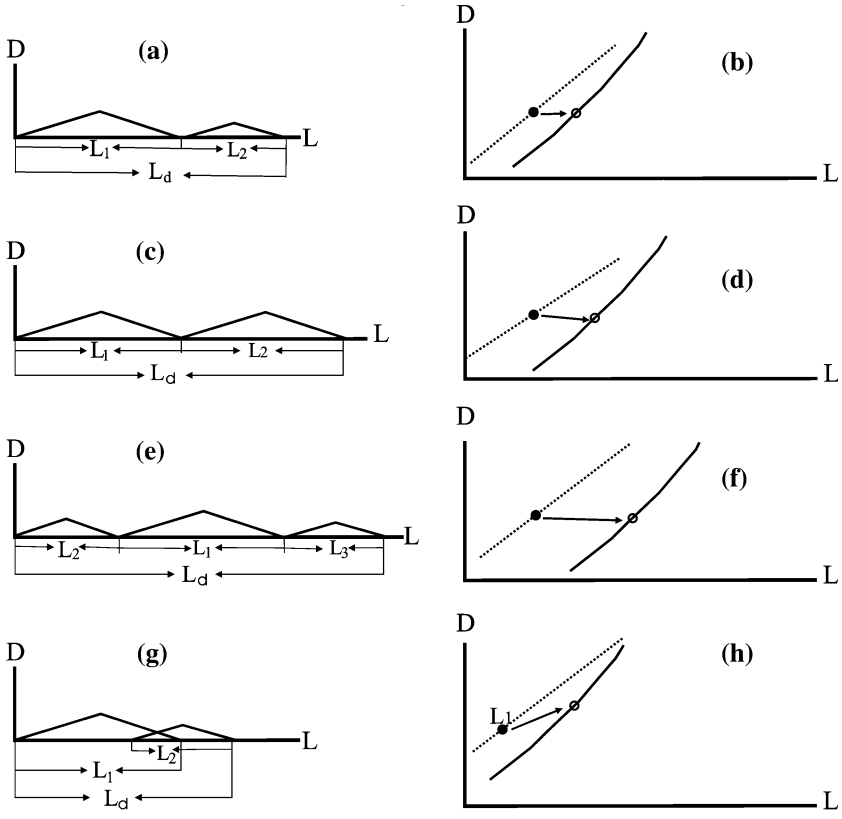

Fig. 5 The deviations of fault length L due to fault linkage depending on fault length and relative location. **a** Two underlapped faults with unequal lengths link each other. **c** Two faults underlapped with equal lengths link each other. **e** Three underlapped faults with unequal lengths link each other. **g**. Two overlapped faults link each other. In (**b**), (**d**), (**f**), and (**h**), the D–L relationship before the linkage is assumed to be 1 (*pointed line*), and the instantaneous D–L relationship after the linkage change is assumed to be non-linear. The *solid circle* shows the position of D/L_1 for fault 1 before linkage. *Open circle* shows the position of the instantaneous value of D/L_d at the beginning of linkage

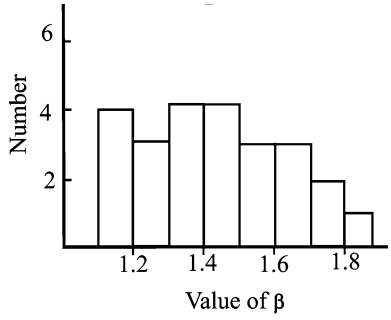

Fig. 6 Frequency of fault size (fault length and displacement) exponents (β values) for two-dimensional data. Data are from Barton and La Pointe (1995), Scholz et al. (1993), Line et al. (1997), Yielding et al. (1996), Needham et al. (1996), and Cladous and Marrett (1996)

by some authors (e.g. Turcotte and Anderson 1992; Yielding et al. 1996). Although different data has been obtained in other experiments (Suteanu et al. 2000), in this paper we adopted a value near the Sammis's model for fault length L distribution using the following equation

$$N \propto L^{-1.6} \tag{3}$$

For the sake of comparison, the standard datasets are constructed by two following equations

$$D = 0.01L \tag{4}$$
$$D = 0.005L. \tag{5}$$

In these two equations, that $c = 0.01$ and $c = 0.005$ selected, respectively, is reasonable, because in most situations, the value of c in Eq. 1 is less than 0.1 (e.g. Dawers et al. 1993; Fossen and Hesthammer 1997). Note that $n = 1$ is assumed for these two equations. The constructed standard datasets are shown in Fig. 7. Dataset E is constructed from Eqs. 3 and 4. E′ is a dataset in which the distribution of fault length is the same as the dataset E but with one difference of order of magnitude. E″ is a dataset in which the distribution of fault length is the same as the dataset E but with the value of c conforming to Eq. 5. The datasets with different distribution of deviations based on the fault length of dataset E are constructed in Fig. 8. In these datasets, relative deviation less than zero indicates that the fault length measured is less than the ideal fault length, and relative deviation larger than zero indicates that the fault length measured is larger than the ideal fault length.

Mathematically, if DPL^n and LPD^m, equation $n = 1/m$ will be true. In practice, we do not know whether D or L is the independent variable. However for a dataset, if $n = 1/m$, we can ignore which of D and L is the independent variable. The difference between n and $1/m$ will be tested in our simulations.

Simulations

We propose five separate models for simulating the deviations of fault length on the relationship between the

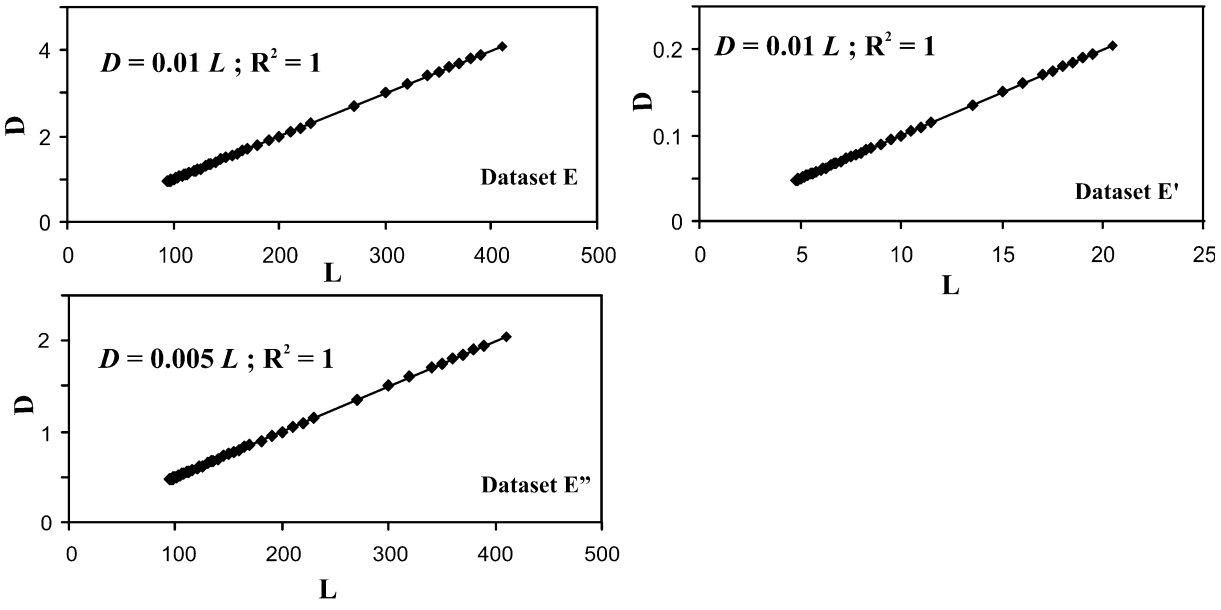

Fig. 7 Constructed standard datasets. L is the length of fault trace. D is the fault displacement. See explanation in the text for the constructed methods

maximum displacement and length and one combined model for simulating effects of combined datasets.

(1) Model 1 includes datasets E_1 to E_3 and it is assumed that the relative deviations for all faults within a dataset are the same and less than zero. The relative deviations of the fault length in these datasets are constructed based on dataset E. The results of simulation for this model indicate that a uniform relative deviation of the fault length does not change the value of n (datasets E_1–E_3 in Table 1) and maintains $n = 1/m$ for any of the datasets. The values of c are larger than the assumed value and increase by increasing the absolute value of λ.

(2) Model 2 includes datasets E_4 to E_8 and it is assumed that absolute deviation of fault length is less than zero and is the same for each fault within the dataset. The absolute length deviations in these datasets are based on the dataset E. This uniform absolute deviation model is consistent with the situation of unresolved tip regions (δ_2, λ_2). Three results (Table 1) are obtained: (a) the deviations of trace length due to unresolved tip regions cause the values of n less than assumed value 1; (b) the values of c increase with increasing absolute deviation. The values of n and correlation coefficient decrease with increasing of absolute value of deviation of fault length; (c) $n \approx 1/m$. These indicate that the deviations of trace length due to unresolved tip regions may cause the value of n to change considerably. The smaller the faults are for a dataset, the larger will be the change in the value of n.

(3) Model 3 includes datasets E_9 to E_{13} and it is assumed that the relative deviations are less than zero and have an arbitrary distribution within the dataset (E_9–E_{13} in Fig. 8). The relay structure may conform to the model. The characteristic of the data for the relay structure is underestimating of trace length (λ_3). The relative deviations are irregular for different faults because the degree of overlapping for each fault is different. The parameter λ_1 in Fig. 2 and λ_4 in Fig. 5g are also consistent with this model. The results of simulation indicate that datasets for model 3 make values of n either larger than or less than the assumed value 1 and $n \neq 1/m$ (Table 1), which depend on the distribution of relative deviations (Fig. 8). The difference between n and $1/m$ is considerably large when R^2 is less than 0.6 as in datasets E_9 and E_{13}. The deviations of c value for datasets E_9 and E_{13} are also large.

(4) Model 4 includes datasets E_{14} to E_{18} and it is assumed that the relative deviations of fault length are larger than zero and have arbitrary distribution within a dataset (E_{14}–E_{18} in Fig. 8). The hard-linked faults in Fig. 5a, c, and e conform to the model, because the characteristic of the data for the hard-linked faults is overestimating of trace length. The relative deviations (λ_4) are not uniform within a dataset since the degree of displacement accumulation after linking is different for each fault. Therefore, the distribution of the deviations is arbitrary. The results of simulation indicate that the datasets for model 4 would make values of n either larger than or less than the assumed value 1 and $n \neq 1/m$ (E_{14}–E_{18} in Table 1), which depends on the distribution of relative deviations (Fig. 8).

(5) Model 5 includes datasets E_{9+14}, E_{10+15}, E_{11+16}, E_{12+17}, E_{13+18}. The model simulates the mixed effects from model 3 and model 4 combined. For example, if the first number of the dataset E_9 has

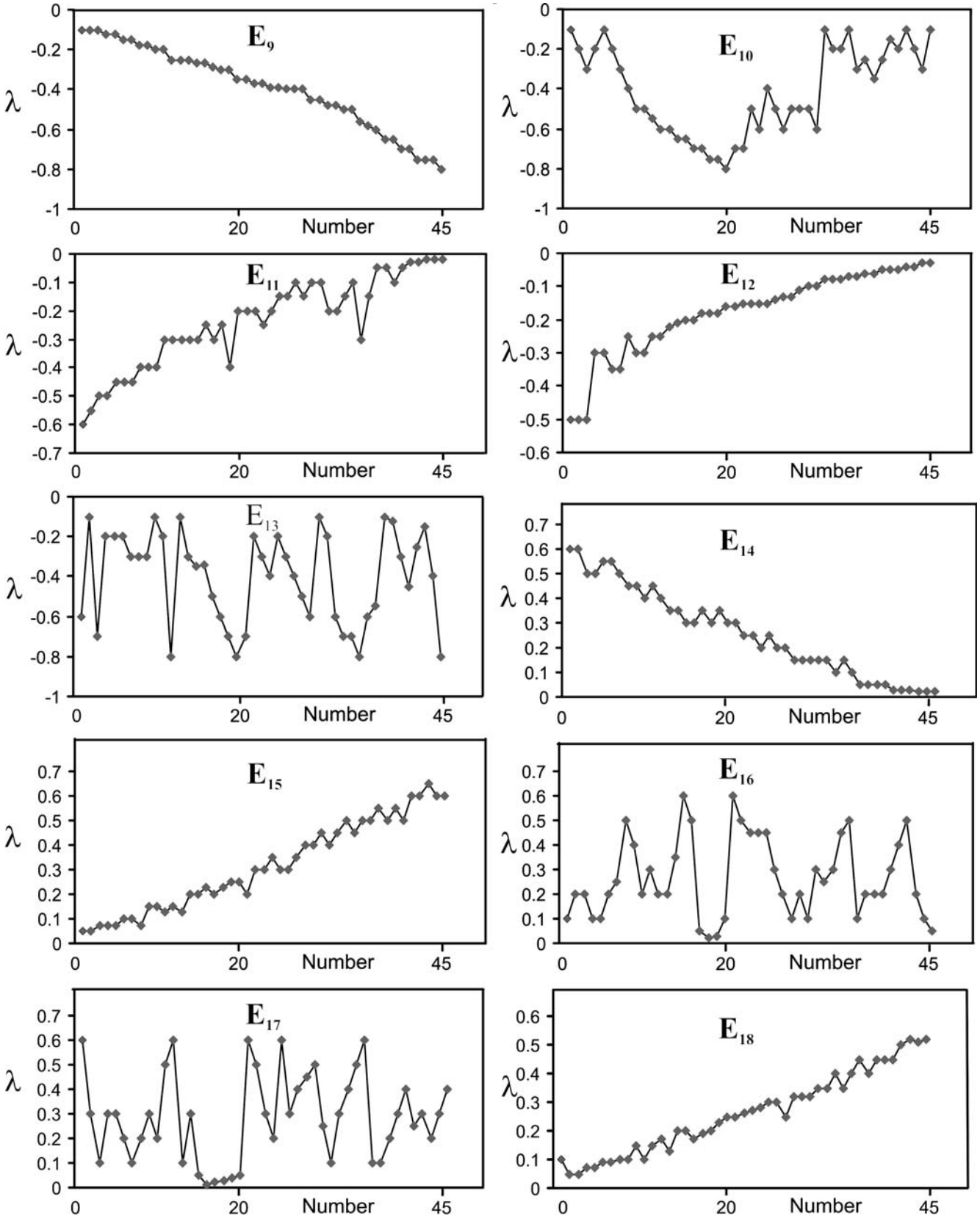

Fig. 8 Constructed relative deviations of fault length based on dataset E. The *ordinate* indicates the relative deviation. The *abscissa* indicates the number within the datasets. Datasets E_9–E_{13} have relative deviations of fault length L less than zero. Datasets E_{14}–E_{18} have relative errors larger than zero comparing fault length L of dataset E

Table 1 Parameters showing datasets constructed according to different deviation types

Dataset	R^2	n	m	$1/n$	$1/n-m$	C
Model 1: datasets with uniform negative relative errors of fault length						
E_1 (−0.2)	1	1	1	1	0	0.0125
E_2 (−0.15)	1	1	1	1	0	0.0118
E_3 (0.3)	1	1	1	1	0	0.0107
Model 2: datasets with uniform negative absolute errors of fault length						
E_4 (−50)	0.9941	0.7046	1.4109	1.4192	0.0088	0.061
E_5 (−40)	0.9969	0.7677	1.2986	1.3026	0.004	0.0419
E_6 (−30)	0.9986	0.8282	1.2056	1.2074	0.0018	0.029
E_7 (−20)	0.9995	0.8869	1.127	1.1275	0.0005	0.0203
E_8 (−10)	0.9999	0.9944	1.0592	1.0593	0.0001	0.0142
Model 3: datasets having relative error of fault length less than zero						
E_9	0.9271	0.5423	1.7097	1.8439	0.1342	0.1398
E_{10}	0.5432	0.5548	0.9791	1.8025	0.8274	0.1354
E_{11}	0.9197	1.6715	0.609	0.5983	−0.0107	0.0005
E_{12}	0.8664	1.4226	0.609	0.7029	0.0939	0.0016
E_{13}	0.5803	0.5069	1.1447	1.9728	0.8281	0.1659
Model 4: datasets having relative error of fault length larger than zero						
E_{14}	0.9955	0.7711	1.2911	1.2968	0.0057	0.0271
E_{15}	0.9818	0.1367	0.7182	0.7315	0.0133	0.0011
E_{16}	0.9287	0.9499	0.9776	1.0527	0.0751	0.0104
E_{17}	0.9168	0.9461	0.9691	1.0569	0.0878	0.0105
E_{18}	0.9891	1.2751	0.7757	0.7842	0.0085	0.0018
Model 5: datasets having mixed relative errors of model 4 and model 5						
E_{9+14}	0.9163	0.4658	1.967	2.1468	0.1798	0.1714
E_{10+15}	0.4369	0.7062	0.6186	1.4160	0.7974	0.0504
E_{11+16}	0.7194	1.1666	0.6167	0.8572	0.2405	0.0043
E_{12+17}	0.7961	1.1011	0.7205	0.9083	0.1878	0.0054
E_{13+18}	0.5408	0.7424	0.7285	1.3469	0.6184	0.0425
Model 6: combined datasets						
E + E′	1	1	1	1	0	0.01
E + E″	0.6629	1.006	0.6589	0.994	0.3351	0.007
E′ + E″	0.9932	0.7977	1.245	1.2536	0.0086	0.0148

R^2, correlation coefficient for log D on log L; n, exponent for log D on log L; m, exponent for log L on log D; E_1–E_3 are datasets with uniform relative deviations of L based on dataset E in Fig. 7. The values in brackets of E_1–E_3 are relative deviations for each fault compared to L for dataset E in Fig. 7; values in brackets from E_4 to E_8 are absolute deviations compared to L of dataset E in Fig. 7. Datasets E_9–E_{18} have relative deviations shown in Fig. 8. E_{9+14} is a dataset with synthetic relative deviation of E_9 and E_{14} (see explanation in the text). Other datasets for model 5 are constructed like in E_{9+14}

relative deviation −0.1 and the first number of the dataset E_{14} has relative deviation −0.6, then the first number of the dataset E_{9+14} has relative deviation of $-0.1+(-0.6)=-0.7$. The relative deviations (λ) in this model would be either negative or positive for different faults within a dataset, therefore the model can be considered as a general model of fault length deviations and represents the data undertaking mixed deviations derived from λ_1 to λ_4. The results of the simulation indicate that synthetic deviations of fault length would cause the values of n either larger than or less than the assumed value 1 (Table 1) depending on the deviation distribution of a dataset and $n \neq 1/m$ in all cases. The difference between n and $1/m$ is quite large when R^2 is less than 0.6 in some datasets such as datasets E_{16+21} and E_{13+18}.

(6) Model 6 is a combined model. The results are shown in Table 1. Three combined methods are used for this model. First, the dataset E + E′ is a combination of datasets with different order of magnitude but the same value of c. This combined dataset does not cause the value of n to change. Secondly, the dataset E + E″ is a combination of datasets with different value of c but the same order of magnitude. This combined dataset causes the value of n to be larger than 1. Thirdly, the dataset E′ + E″ is a combination of datasets both with different order of magnitude and different value of c. This combined dataset causes the value of n to be less than 1. These results indicate that the combined datasets only from those datasets having the same distribution of fault length and value of c does not cause deviations of the values of n.

Value of *n* estimated from previous datasets in literature

Collected datasets

Nineteen previous datasets are collected for calculating the value of n. Some datasets are directly obtained from numerical values published in the literature. Other datasets are obtained from the published numerical plots. The faults used from the literature may be strike-

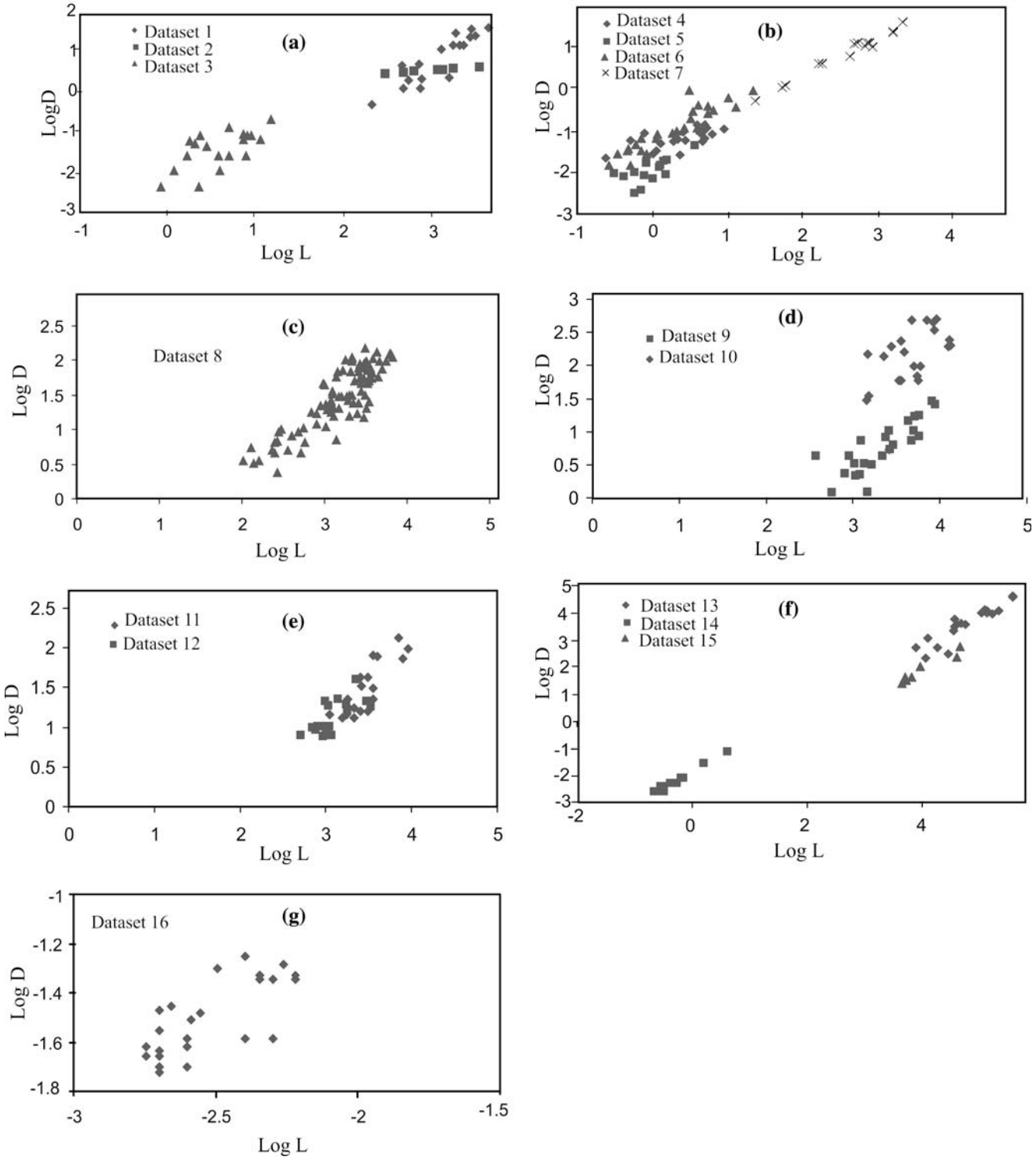

Fig. 9 Logarithmic plots of displacement versus trace length for individual datasets derived from published literature. *L* and *D* are in meters. Dataset 1 is from Krantz (1988); dataset 2 from Opheim and Gudmundsson (1989); dataset 3 from Peacock and Sanderson (1991); dataset 4 from Peacock (1991); dataset 5 from Muraoka and Kamata (1983); dataset 6 from Villemin et al. (1995); dataset 7 from Dawers et al. (1993); dataset 8 from Cartwright et al. (1995); dataset 9 from Gudmundsson (2000); dataset 10 from Poulimenos (2000); dataset 11 from Nicol et al. (1996); dataset 12 from Watterson (1986); dataset 13 from Elliot (1976); dataset 14 from Wilkins et al. (2001); dataset 15 from Barnett et al. (1987); dataset 16, from Lu et al. (1989)

slip, thrust or normal with the fault magnitudes from 10^{-2} to 10^{5} m, spanning eight orders of magnitude. The smallest fault lengths come from the physical experimental data (Lu et al. 1989). The largest fault magnitudes are cited from Elliot (1976). Some literature published both numerical values and numerical plots, on

the behalf of this advantage we tested that the absolute errors of value of n from individual datasets of the published numerical plots are less than 0.06. Most datasets except datasets 17, 18, 19 are shown in the log–log plots in Fig. 9. The datasets were selected on the following principles. Each dataset comes from an individual tectonic setting or the same tectonic domain. Those mixed datasets are not included. The correlation coefficient (R^2) for each dataset is larger than 0.6. Most points can be distinguished on the plots if the datasets are from numerical plots published.

Analysis of the results

For a dataset, if $n = 1/m$, we can ignore whether D or L is the independent variable. Either $n = 1/m$ or $n \neq 1/m$ will be tested in the analysis. For a dataset, if $n \neq 1/m$, the method of double regression is used to estimate values of n, which may minimize the product of deviations in L and D (Davis 1986; Gillespie et al. 1992). The results are shown in Table 2. The main characteristics of these datasets are:

(1) All individual datasets show $n \neq 1/m$, which indicates the individual datasets always contain deviations and the distribution of the relative deviations are not uniform.
(2) Dataset 7 (Dawers et al. 1993) and dataset 14 (Wilkins et al. 2001) have minimum differences between n and $1/m$ and have high correlation coefficients. Dataset 7 is from relatively homogeneous rocks and better outcrop in studied area and dataset 14 is formed completely by isolated faults. These results indicate that the datasets formed in a single tectonic environment with uniform mechanical properties by isolated faults have minimum deviation of fault length.
(3) The values of n for different datasets are either larger or less than 1, the maximum value of n is not larger than 1.5.
(4) The average n_d for double regression is 1.0813 for all collected datasets. This value is very close to 1.
(5) Histogram of values of n_d (Fig. 10) shows that the peak of n_d is in the range 1.0–1.1. This value is also close to 1.The above results imply the real value of n is close to 1 and the relationship of length–displacement in a single tectonic environment with uniform mechanical properties should be linear. These results are consistent with the conclusions of Clark and Cox (1996) who analyzed 11 previous datasets and found a linear relationship between fault displacement and length.

Value of *n* estimated from size distributions of faults

Power-law distribution of fault size (displacement and length) has been proposed by many authors (e.g. Marrett and Allmendinger 1991; Watterson et al. 1996). For maximum displacement, an equation can be expressed as

$$N \propto D^{-\beta 1}. \tag{6}$$

For fault length,

$$N \propto L^{-\beta 2}. \tag{7}$$

Table 2 Parameters showing individual datasets

Dataset	Number	a-log L	a-log D	R^2	n	m	$1/n$	n_d
1	16	3.0896	0.755	0.7443	1.4441	0.5154	0.6925	1.6051
2	7	2.9857	1.13	0.9653	0.6434	1.5001	1.5542	0.6547
3	20	0.6354	−1.4078	0.8045	0.8087	0.5831	1.2366	1.2415
4	20	0.3795	−1.2325	0.4448	0.3801	1.1703	2.6308	0.6614
5	15	0.0246	−1.9359	0.6261	0.9214	0.6795	1.0853	1.1645
6	26	0.3195	−1.0022	0.8863	0.9023	0.9822	1.1083	0.9186
7	15	2.5844	0.7445	0.9757	0.8871	1.0997	1.1273	0.8981
8	92	3.1822	1.4811	0.9591	0.9237	0.814	1.085	1.0933
8-1	23	3.1761	1.4654	0.668	0.888	0.7523	1.1261	1.3815
8-2	69	3.1842	1.4864	0.7883	0.9379	0.8405	1.0662	1.0563
9	24	3.3333	0.7583	0.68	0.8588	0.7919	1.1644	1.0042
10	22	3.528	2.2785	0.816	0.8788	0.9254	1.1379	0.9021
11	68	0.404	−2.6439	0.7456	0.5102	1.5277	1.96	0.5651
12	18	3.1139	1.1742	0.6137	0.8063	0.7133	1.2402	1.0646
13	19	4.7301	3.5752	0.8466	1.2387	0.6824	0.8073	1.3468
14	11	−0.2688	−2.1957	0.9661	1.2105	0.7981	0.8261	1.23157
15	7	3.9831	1.8856	0.9256	1.1246	0.8234	0.8892	1.1684
16	26	−1.4907	−2.4990	0.6	0.8872	0.6466	1.1271	1.02
17	552	2.65	0.01	0.62	0.9	2.37	1.1111	1.46
18	13	3.81	2.31	0.95	1.19	1.32	0.8403	1.25
19	62	1.26	−0.15	0.99	1.0	1.03	1	1.02
Average								1.0813

R^2, regression correlation coefficient for log D on log L; a-log L, average value of log L, a-log D, average value of log D; n, value of n for log D on log L; m, value of n for log L on log D; n_d, value of n for double regression. Datasets 1–16 are the same as on Fig. 9. Datasets 17–19 are relevantly cited from data 1, data 7 and data 10 of Gillespie et al. (1992). The unit of L and D is in meters

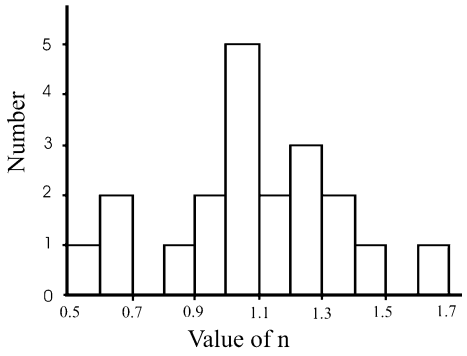

Fig. 10 Histogram of power-law exponent (n) for $D = cL^n$ based on the data in Table 2

Here, the significance of N, L, D, $\beta1$, $\beta2$ can be referred to in Eq. 2. From Eqs. 6 and 7, we can obtain

$$L^{-\beta2} \propto D^{-\beta1}. \tag{8}$$

Combining Eqs. 1 and 8, we get

$$n = \frac{\beta2}{\beta1}. \tag{9}$$

Equation 9 shows that the value of n can be calculated if the maximum displacement and trace length populations are given. But the equation is valid only for faults that show no fault displacement or length deviations (Marrett and Allmendinger 1991). Not much literature concerns all the values of n, $\beta2$ and $\beta1$ available to test Eq. 9. The data from Pickering et al. (1996) show values of n may be larger than $\beta2/\beta1$ (number 1 in Table 3) or less than $\beta2/\beta1$ (number 2 in Table 3) due to different deviations. We also can see that the values of n may be larger than 1 (number 1 in Table 3) or less than 1 (numbers 1 and 4 in Table 3) due to different deviations. The power-law exponent (n) changes largely due to the deviations of fault length or displacement for the observed level in map view, unresolved fault tip, fault linkage, etc.

Discussion

When the distribution of relative deviations of a fault population is irregular, the decrease or increase in values of n will depend on the distribution of relative deviations. Figure 11 shows the diagram of this effect. The relationship between the maximum displacement and fault for a dataset with no deviations is assumed to be linear. Figure 11a and b indicates different distribution of deviated fault length. In the case of Fig. 11a, the power-law exponent is larger than 1 and in the case of Fig. 11b, the power-law exponent is less than 1.

Table 3 Comparison between value of n and $\beta2/\beta1$ from size population of faults from the southern North Sea (Pickering et al. 1996, numbers 1, 2, and 3) and southern Utah (Fossen and Hesthammer 1997, number 4)

Number	$\beta1$ value	$\beta2$ value	n	$\beta2/\beta1$
1	2.7	2.01	0.8	0.7444
2	2.7	2.77	1.0	1.0259
3	2.7	4.11	1.5	1.5222
4	0.9	0.6	0.54	0.6667

The collected datasets in this paper do not include those datasets with a large amount of faults that may be as good as or better than the datasets selected for analyzing the value of n. Three of these are shown in the Fig. 1 in Marrett and Allmendinger (1991), which includes the dataset of Gulf of Mexico containing 242 faults, the dataset with 136 faults cited from MacMillan (see reference of Marrett and Allmendinger 1991) and the dataset with 130 faults cited from MFRG (see the reference of Marrett and Allmendinger 1991). Two other datasets are measured by Mansfield and Cartwright (2001) using physical modeling and that measured by Schlische et al. (1996) in the Mesozoic Dan River rift basin. The former contains 237 faults. A value $n = 0.93$ is obtained for this data, which is also close to 1. The latter contains 201 faults. The best-fit power-law curve has an exponent of 0.914, which is nearly linear. The data published by Lu et al. (1989) and Wen et al. (1990) also indicate that value of n is equal to 1. So we think that excluded datasets would not influence our basic results.

Many previous experiment and fieldwork data have shown that n should be equal to 1 (e.g. Gudmundsson 1987; Gillespie et al. 1992; Lu et al. 1989; Wen et al. 1990; Dawers et al. 1993), which can be predicted by Dugdale's model of fracture (Cowie and Scholz 1992a, b). Dugdale's fault growth model indicated that the deformation at the tip of a tensile crack in an elastic-plastic material is inelastic deformation. This model predicts linear relationship between displacement and length of fault:

$$D = \frac{C(\sigma_0 - \sigma_f)L}{\mu} \tag{10}$$

where σ_0 is the shear strength of the surrounding rock, μ the shear modulus, σ_f the frictional shear stress on the fault, C a constant (Cowie and Scholz 1992a). Therefore, there is a theoretical base for assuming $n = 1$. It is reasonable to consider that the relationship between maximum displacement and fault length is linear (Sneddon and Lowengrub 1969).

For this paper, only deviations of fault length are considered for the simulations. In practice, there would exist deviations of displacement due to sampling and physical process of faulting. Therefore, real deviation distribution within a dataset is more complicated than that considered in this paper.

Besides the fault linkage, the mechanical properties of host rocks also influence the development of faults. Anisotropy and heterogeneity such as mechanical layering have very large effects on the stress fields and these stress fields control fault formation (e.g. Gross et al.

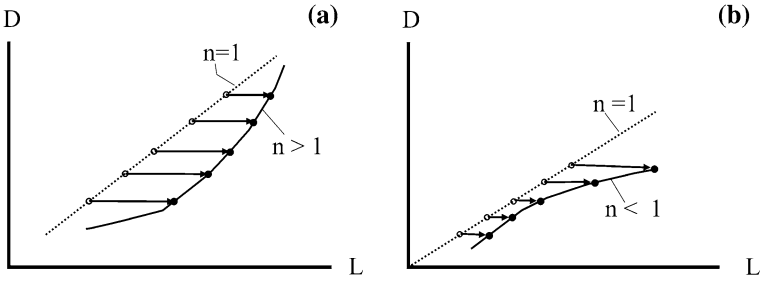

Fig. 11 Diagram showing the influence of distribution of deviations of fault trace length within a dataset. The *pointed line* indicates the *D–L* relationship with no deviations of fault length. The *solid line* indicates the *D–L* relationship with deviations of fault length. See explanation in the text

1997; Bai et al. 2000). Gudmundsson (2004) proposed that Young's modulus affects fault formation both spatially and temporally. The deviations of fault length caused by the mechanical properties can be simulated by model 5.

Conclusions

The value of n is related to the faulting mechanism, therefore it is important to determine the value of n. However in many cases, the value of n is obtained from individual data which could not represent the real value of n. In this paper, the effects of the errors and uncertainties related to deviation of the displacement–length relationship for faults are quantitatively simulated. We examined 19 datasets as earlier studies, which have been the bases of a dispute about the values of n, in particular whether the value of n is close to 1 or deviates much from 1.

Based on $n=1$, the numerical simulations were done and the following conclusions are drawn.

(a) Uniform relative deviations of fault length would not change the value of n.
(b) Uniform absolute deviations of fault length due to unresolved fault tips may decrease the value of n, and the deviation of values of n increase by the length absolute deviations.
(c) The relative deviations of fault length due to fault linkage and observed dimension of faults may be larger than or less than zero, which either increases or decreases the values of n depending on the distribution of relative deviations of fault length within a dataset.
(d) The mixed deviations of fault length may be either less than or larger than zero, and either increases or decreases values of n depending on the distribution of deviations of a dataset.
(e) A combined dataset from the datasets with different value of c and orders of magnitude also cause the values of n to deviate. Therefore combined data is not appropriate to obtain the power-law exponent for *D–L* relationship.Data spanning eight orders of magnitude are collected from the published literature. The values of n_d for double regression range from 0.55 to 1.65 and the average value of n_d is 1.0813 and the peak n is in the range 1.0–1.1. These results imply that the real value of the power-law exponent (n) of the relationship between maximum displacement and fault trace length should be equal to 1. The relationship can be explained by Dugdale's model. A non-linear relationship for *D–L* implies that the shear strength of the surrounding rock (σ_0) varies with fault size. However there is no physical basis supporting it. The large scatter of *D–L* plots may result from deviations of trace length due to the observed level in map view, unresolved fault tip, fault linkage etc.

Acknowledgements This work was supported by projects D.01003, F30617 of the Mexican Institute of Petroleum and CONACYT-33087-T, PAPIIT IN102602-3. This manuscript benefited greatly from thorough reviews by Agust Gudmundsson and Jorn H. Kruhl. We are also thankful for helpful suggestions of improvement by N.H. Dawers and Conrad Childs.

References

Acocella V, Gudmundsson A, Funiciello R (2000) Interaction and linkage of extension fractures and normal faults: examples from the rift zone of Iceland. J Struct Geol 22:1233–1246
Bai T, Pollard DD, Gao H (2000) A new explanation for fracture spacing in layered materials. Nature 403:753–756
Barnett JM, Mortimer J, Rippon JH, Walsh JJ, Watterson J (1987) Displacement geometry in the volume containing a single normal fault. Am Assoc Pet Geol Bull 71:915–937
Barton CC, La Pointe PR (1995) Fractals in the Earth sciences. Plenum, New York, pp 262
Bonnet E, Bour O, Odlin NE, Davy P, Main I, Cowie P, Berkowitz B (2001) Scaling of fracture systems in geological media. Rev of Geophys 39:347–383
Cartwright JA, Trudgill BD, Mansfield CS (1995) Fault growth by segment linkage: an explanation for scatter in maximum displacement and trace length data from the Canyonlands Grabens of SE Utah. J Struct Geol 17:1319–1326
Childs C, Watterson J, Walsh JJ (1995) Fault overlap zones within developing normal fault system. J Geol Soc Lond 152:535–549
Cladous TT, Marrett R (1996) Are fault growth and linkage models consistent with power-law distributions of fault lengths? J Struct Geol 18:281–293
Clark RM, Cox SJD (1996) A modern regression approach to determining fault displacement–length scaling relationships. J Struct Geol 18:147–151
Cowie PA, Scholz CH (1992a) Displacement–length scaling relationship for faults: data synthesis and discussion. J Struct Geol 14:1149–1156
Cowie PA, Scholz CH (1992b) Physical explanation for the displacement–length relationship for faults using a post-yield fracture mechanics model. J Struct Geol 14:1133–1148

Crider JG, Pollard DD (1998) Fault linkage: three-dimensional mechanical interaction between echelon normal faults. J Geophys Res 103:24373–24391
Davis JC (1986) Statistics and data analysis in geology. Wiley, New York, pp 646
Dawers NH, Anders MH (1995) Displacement–length scaling and fault linkage. J Struct Geol 17:607–614
Dawers NH, Anders MH, Scholz CH (1993) Growth of normal faults: displacement–length scaling. Geology 21:1107–1110
Elliot D (1976) The energy balance and deformation mechanism of thrust sheets. R Soc Lond Philos Trans Ser A 283:289–312
Ferrill DA, Stamatakos JA, Sims D (1999) Normal fault corrugation: implications for growth and seismicity of active normal faults. J Struct Geol 21:1027–1038
Fossen H, Hesthammer J (1997) Geometric analysis and scaling relations of deformation bands in porous sandstone. J Struct Geol 19:1479–1493
Gillespie P, Walsh JJ, Watterson J (1992) Limitations of displacement and dimension data from single faults and the consequences for data analysis and interpretation. J Struct Geol 14:1157–1172
Gross MR, Gutierrez-Alonzo G, Bai T, Wacker MA, Collinsworth KB, Behl RJ (1997) Influence of mechanical stratigraphy and kinematics on fault scaling relations. J Struct Geol 19:171–183
Gudmundsson A (1987) Tectonics of the Thinvellir Fissure Swarm, SW Iceland. J Struct Geol 9:61–69
Gudmundsson A (2000) Fracture dimensions, displacements and fluid transport. J Struct Geol 22:1221–1231
Gudmundsson A (2004) Effects of Young's modulus on fault displacement. CR Geosci 336:85–92
Gudmundsson A, Brynjolfsson S, Jonsson MTh (1993) Structural analysis of a transform fault-rift zone junction in North Iceland. Tectonophysics 220:205–221
Gupta A, Scholz CH (2000) A model of normal fault interaction based on observations and theory. J Struct Geol 22:865–879
Huggins P, Watterson J, Walsh JJ, Childs C (1995) Relay zone geometry and displacement transfer between normal faults recorded in coal-mine planes. J Struct Geol 17:1741–1755
Krantz RW (1988) Multiple fault sets and three-dimensional strain: theory and application. J Struct Geol 10:225–237
Line CER, Snyder DB, Hobbs RW (1997) The sampling of fault populations in dolerite sills of Central Sweden and implications for resolution of seismic data. J Struct Geol 19:687–699
Lu S, Wen C, Xu S-S (1989) The structural model experiment and mechanism of Nanyang depression. Earthscience 1989(Suppl):97–106
Mansfield C, Cartwright J (2001) Fault growth by linkage: observations and implications from analog models. J Struct Geol 23:745–763
Marrett R, Allmendinger RW (1991) Estimates of strain due to brittle faulting: sampling of fault populations. J Struct Geol 13:735–737
Muraoka H, Kamata H (1983) Displacement distribution along minor fault traces. J Struct Geol 5:483–495
Needham T, Yielding G, Fox R (1996) Fault population description along minor fault traces. J Struct Geol 18:155–167
Nicol A, Walsh JJ, Watterson J, Bretan PG (1996) Three dimensional geometry and growth of conjugate normal faults. J Struct Geol 17:847–862
Opheim JA, Gudmundsson A (1989) Formation and geometry of fractures, and related volcanism, of the Krafla fissure swarm, northeast Iceland. Bull Geol Soc Am 101:1608–1622
Peacock DCP (1991) Displacement and segment linkage in strike slip fault zones. J Struct Geol 13:721–733
Peacock DCP, Sanderson DJ (1991) Displacement and segment linkage and relay ramps in normal fault zones. J Struct Geol 13:721–733
Peacock DCP, Sanderson DJ (1994) Geometry and development of relay ramps in normal fault zones. Am Assoc Pet Geol 78:147–165
Pickering G, Peacock DCP, Sanderson DJ, Bull JM (1996) Modeling tip zones to predict the throw and length characteristics of faults. Am Assoc Pet Geol 80:82–98
Poulimenos G (2000) Scaling properties of normal fault populations in the western Corinth Graben, Greece: implication for fault growth in large strain setting. J Struct Geol 22:307–322
Sammis C, King G, Biegel R (1987) The kinematics of gouge deformation. Pure Appl Geophys 125:777–812
Schlische RW, Young SS, Ackermann RV (1996) Geometry and scaling relations of a population of very small rift-related normal faults. Geology 24:683–686
Scholz CH, Dawers NH, Yu J-Z, Anders MH (1993) Fault growth and fault scaling laws: preliminary results. J Geophys Res 98:21951–21961
Suteanu C, Zugravescu D, Munteanu F (2000) Fractal approach of structuring by fragmentation. Pure Appl Geophys 157:539–557
Sneddon IN, Lowengrub M (1969) Crack problems in the classical theory of elasticity. Wiley, New York, pp 221
Turcotte DL, Anderson A (1992) Fractals in geology and geophysics. Pure Appl Geophys 131:171–196
Villemin T, Angelier J, Sunwoo C (1995) Fractal distribution of fault length and offsets: implication of brittle deformation evolution—the Larraine Coal Basin. In: Barton C, LaPointe P (eds) Fractals in the Earth sciences. Plenum, New York, pp 205–226
Walsh JJ, Watterson J (1988) Analysis of the relationship between displacements and dimensions of faults. J Struct Geol 10:239–247
Walsh JJ, Watterson J (1989) Displacement gradients on fault surface. J Struct Geol 11:307–316
Walsh JJ, Watterson J (1991) Geometry and kinematic coherence and scale effects in normal fault systems. In: Roberts AM, Yielding G, Freeman B (eds) The geometry of normal faults. Geol Soc London Spec Pub 56:193–203
Watterson J, Walsh JJ, Gillespie A, Easton S (1996) Scaling systemics of fault sizes on a large scale range fault map. J Struct Geol 18:199–214
Watterson J (1986) Fault dimensions, displacements and growth. Pure Appl Geophys 124:365–373
Wen C, Lu S, Xu S-S (1990) A study of the syngenetic faults of Nanyang depression. Geoscience 4:46–54
Wilkins SJ, Gross MR, Wacker M, Eyal Y, Engelder T (2001) Fault joints: kinematics, displacement–length scaling relations and criteria for their identification. J Struct Geol 23:315–327
Willemse EJ, Pollard DD, Aydin A (1996) Three-dimensional analysis of slip distributions on normal faults arrays with consequence for fault scaling. J Struct Geol 18:295–309
Yielding G, Needham T, Jones H (1996) Sampling of fault populations using sub-surface data: a review. J Struct Geol 18:135–146
Xu S-S, Li D, Wen C (1998) Fault characteristics of Nanyang depression. Explor Geosci 13:94–99